Electronic Journal of Polish Agricultural Universities is the very first Polish scientific journal published exclusively on the Internet, founded on January 1, 1998 by the following agricultural universities and higher schools of agriculture: University of Technology and Agriculture of Bydgoszcz, Agricultural University of Cracow, Agricultural University of Lublin, Agricultural University of Poznan, Higher School of Agriculture and Teacher Training Siedlce, Agricultural University of Szczecin, and Agricultural University of Wroclaw.

ELECTRONIC JOURNAL OF POLISH AGRICULTURAL UNIVERSITIES

2007
Volume 10
Issue 4
Topic
GEODESY AND CARTOGRAPHY

TROJANOWICZ M. 2007. LOCAL MODELING OF QUASI-GEOID HEIGHTS ON THE STRENGTH OF THE UNREDUCED GRAVITY AND GPS/LEVELING DATA, WITH THE SIMULTANEOUS ESTIMATION OF TOPOGRAPHIC MASSES DENSITY DISTRIBUTION
EJPAU 10 (4), #35.
Available Online http://www.ejpau.media.pl/volume10/issue4/art-35.pdf

LOCAL MODELING OF QUASI-GEOID HEIGHTS ON THE STRENGTH OF THE UNREDUCED GRAVITY AND GPS/LEVELING DATA, WITH THE SIMULTANEOUS ESTIMATION OF TOPOGRAPHIC MASSES DENSITY DISTRIBUTION

Marek Trojanowicz
Institute of Geodesy and Geoinformatics,
Wrocław University of Environmental and Life Sciences, Poland

ABSTRACT

One of the problems occurring in the classical methods of geoid and quasi-geoid altitude determination, which lower their accuracy, is the necessity to implement various corrections to the input data. The other important issue in a precise geoid determination is the recognition of topographical masses density distribution. Its variations are significant and could reach one centimeter - even for a slightly folded terrain. The paper suggests the method for the quasi-geoid altitude modeling on the basis of non-reduced surface gravity data and heights anomalies of the GPS/leveling. The method depends on generating a disturbing potential model whose component is the topographical masses density distribution model.
The paper presents preliminary examination results performed in the test area located in Lower Silesia, SW Poland. The achieved precision of calculated quasi-geoid heights is about ±1.7 cm in the meaning of a mean square error. Attained precision of the model is close to the accuracy of a test, GPS/leveling data. Good results were obtained within the range of about 20 km from the border of the area covering a gravity data. It confirms that the proposed solution could be used in case of lack of the gravity data on large regions outside the examined area. The designated model of topographic masses density confirms that such solution allows to interpolate height anomalies and model topographic masses density at the same time.

Key words: neural networks, sets of neural networks, evaluation of quality, generalization error, forecast the value of space

INTRODUCTION

There are many ways of geoid and quasi-geoid determination. A general overview of these methods may be found in [8,9,19,29,33]. Principally, there are two common groups of methods to mention [29]: least-squares approximation (with least-squares collocation as the most popular) and the methods based on the Stokes integral.

Taking into account the data set used in a calculation process, it should be noticed that Stokes integration methods are generally based on gravity anomaly data. Approximation methods can use mixed data types like gravity gradients, GPS/leveling data, gravity anomalies and disturbances [31]. If we consider data quantity, we realize that the base of precise calculations for both groups are gravity data. Gravimetric geoid or quasi-geoid have systematic offset and tilt in reference to GPS/leveling data, caused by the long-wavelength errors of geoid or quasi-geoid and systematic errors of both leveling and GPS data [31]. Consequently, in order to be applicable in satellite leveling in a national height system, such kind of geoid or quasi-geoid should be adjusted to GPS/leveling data. Hence, the data set commonly used in calculation process should be completed by GPS/leveling data.

Making calculations according to the above mentioned classical solutions is difficult which is noticeable especially in the case of the mountainous areas, if the purpose of these calculations is to determine the geoid or quasi geoid model with the accuracy of 1cm. These difficulties result mainly from the necessity of implementing certain reductions and corrections to the input data (mainly topographic correction) that follow detailed solutions of this method. These corrections as well some approximations that occur in classical solutions were the subject of many analyses and comparisons. They were discussed in the recently published papers: [1,11,17,18,20,21,22,23,24,25,32]. These studies suggest that determining the geoid with 1 cm accuracy requires not only very precise data (gravimetric data and digital terrain model) but also the modification of the present classical techniques for the geoid and quasi-geoid determination or searching the new methods.

The other disturbing factor, which accompanies the task of geoid determination, is unacquaintance of topographic masses density distribution. In practice the constant density is mostly used (e.g. $\rho = 2670 \,\mathrm{kg} \cdot \mathrm{m}^3$). However, a real density can significantly differ from this constant value. These variations can implement errors into the reduced gravity and the calculated geoid heights. Such problem was studied also in recent years [1,10,14,22]. Sjöberg [22] pointed out that density variations could be in the range of centimeters for topographic elevations above 660 m. For elevations of 1000*m*, 2000*m* and 5000*m* the effect could reach the values of ±22, ±8.8 and ±56.8 cm. This information can be taken from all available sources like geological maps, seismic and borehole measurements, density rocks Tables etc. [14]. Topographic masses density may be determined also on the basis of data used for the geoid or quasi-geoid designation (gravimetric anomalies and GPS/levelling data). In this case, this data would be crucial in the process of the Earth gravity field modelling both in geodetic and in the geophysical sense.

With reference to all these issues, the main purpose of this elaboration is suggesting the method for quasi-geoid determination that minimizes problems connected with introducing corrections to the input data. This method eliminates such problems because the input data is not reduced. The suggested solution is based on a disturbing potential model which includes the model of topographical masses density distribution. To some extent, it is the solution of the second problem mentioned above, namely determination of topographic masses density.

Gravimetric data and heights anomalies determined from GPS measurements on points whose normal heights are known, are the basis for calculations.

The proposed solution should be perceived as a kind of solution for gravimetric inverse problem. In relation to this, the solution of the task as such may be found using techniques of gravity field inversion [4, 26, 27].

DISTURBING POTENTIAL MODEL

This section presents the suggested disturbing potential model and the way of estimating its parameters.
Let's consider a point *P* situated on the terrain surface (Fig. 1). The disturbing potential in this point can be divided into three components:

potential T_Ω produced by topographic masses Ω laid above the geoid, with density distribution function ρ .

potential T_κ produced by disturbing masses κ occurring under the geoid surface with density distribution function δ .

potential T_r which represents the remaining influences.

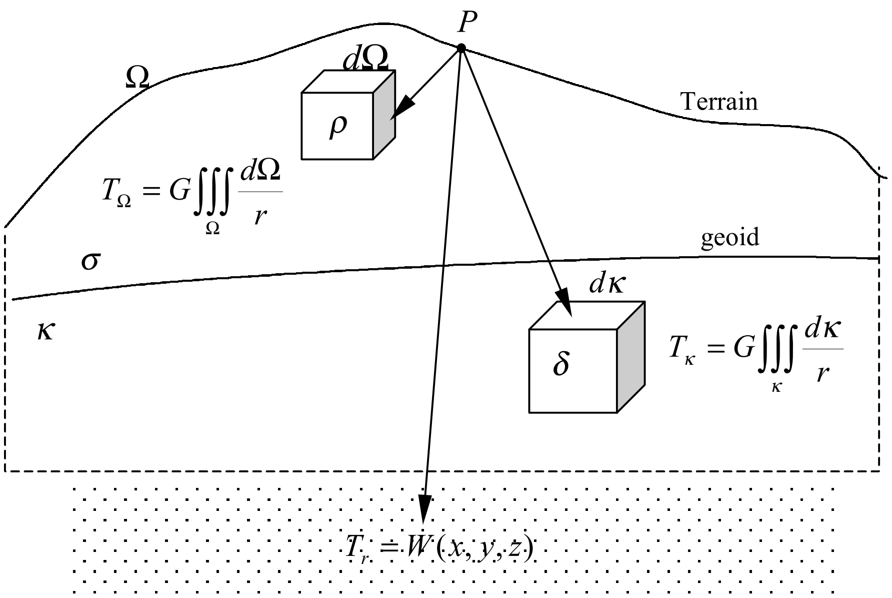

Fig. 1. Disturbing potential model

Potentials T_Ω and T_κ produced by masses Ω and κ are defined by Newton's integral and expressed respectively:

$$T_\Omega = G\iiint_\Omega \frac{d\Omega}{r} = G\iiint_\Omega \frac{\rho}{r} dV_\Omega \tag{1}$$

$$T_\kappa = G\iiint_\kappa \frac{d\kappa}{r} = G\iiint_\kappa \frac{\delta}{r} dV_\kappa \tag{2}$$

where *G* is the Newton's gravitational constant, dV_Ω and dV_κ are elements of volume, *r* is the distance between the attracting masses and the attracted point *P*.

Due to the fact that Ω and κ regions cover limited area of interest, the potential T_r contains influences of disturbing masses which lay outside the regions, and are not included in two preceding components. Furthermore, its role is to link the gravity and the GPS/leveling data, so it has to cover an offset and a tilt between gravimetric quasi-geoid and GPS/leveling data. Both mentioned roles of the potential T_r can be considered as a long wavelength. Hence, the potential can be represented for instance by harmonic spherical polynomials of a low degree.

Finally, the disturbing potential on the terrain surface can be written as:

$$T_P = T_r + T_\Omega + T_\kappa \tag{3}$$

The synthetic form of disturbing potential (3) allows to formulate a gravity inversion task as the one that requires to: *find such functions of density distribution ρ and δ inside the defined regions Ω and κ to satisfy the equality of the disturbing potential values given by equation (3) and its other quantities to their real values on survey points..*

This task may be solved by making continuous volume functions ρ and δ discrete. To do so, Ω and κ regions have to be divided into finite volume blocks and the constant density has to be assigned to each of the blocks. Densities of the blocks now become the searched values.

The division of the Ω region, basically may be defined by digital terrain model (DTM), if we assume the constant density of topographic masses for the single block from the geoid to the terrain surface. Due to the fact that determining the density for each DTM block separately, when the DTM resolution is high, would involve determining the great amount of unknown values, it seems reasonable to group DTM blocks in the zones that have the same density. If such assumption was taken, the constant searching for density ρ_k would refer to all DTM blocks situated in *k* zone.

The κ region may be treated as the slab with the same thickness. The division into blocks at the constant density δ_j would be the set consisting of one or many layers of spherical or rectangular prisms - depending on the adopted coordinate system.

Considering gravimetric data that are the basis of calculations, the influence of Ω and κ regions may be treated as the topographic-isostatic correction. The borders of these regions may be described using guidelines that direct calculation of topographic-isostatic reduction of the gravity data. Because the model (3) contains the component T_r, so the analogy that facilitates finding the border of Ω and κ regions is only a suggestion and can define maximum range of these areas. So in the horizontal plane, these regions should go behind the border of data occurrence. It also seems reasonable to take that the κ region thickness is approximately equal to the *T* - depth of the compensation surface. Precise determination of these regions values certainly demands many calculation tests.

When Ω and κ regions are defined in such a way, the potential (3) may be described as a linear function of the searched parameters, which are ρ_k and δ_j densities, and as coefficients of the polynomial that approximates T_r potential.

If calculations are made in spherical coordinates, T_r potential can be approximated with harmonic spherical polynomials of a low degree, so we can generally write:

$$T_r(\phi_P, \lambda_P, R_P) = W(\phi_P, \lambda_P, R_P) = \mathbf{w}^{\mathbf{T}}\mathbf{a} \tag{4}$$

where

ϕ_P, λ_P, R_P – spherical coordinates of the attracted point *P*,

$\mathbf{a}^{\mathbf{T}} = [a_1, ..., a_l]$ is the vector of polynomials coefficients a_u (*u=1...l*),

$\mathbf{w}^{\mathbf{T}} = [w_1, ..., w_l]$ comes from the form of taken polynomials.

Recording T_Ω potential requires geoid approximation by a sphere with the mean Earth's radius R_b. The component T_Ω is determined on the strength of Ω region defined as a rectangular spherical grid of DTM, where particular block *i* is a spherical prism limited by spheres with a radius R_b - at the bottom and $R_{ti} = R_b + H_i$ - at the top.

T_Ω potential can be written as:

$$T_\Omega\left(\phi_P, \lambda_P, R_P\right) = G\sum_{k=1}^{n}\left(\rho_k \sum_{i=1}^{m_k} \int_{R_b}^{R_b+H_i} \int_{\phi_{1i}}^{\phi_{2i}} \int_{\lambda_{1i}}^{\lambda_{2i}} \frac{R_i^2 \cos\phi_i}{\sqrt{R_i^2 + R_P^2 - 2R_i R_P \cos\psi_i}} d\lambda_i d\phi_i dR_i\right) = \mathbf{t}^{\mathbf{T}}\boldsymbol{\rho} \tag{5}$$

where

n – number of DTM zones (there will be calculated constant density ρ_k for each zone),

m_k – number of spherical prisms of DTM in zone *k*,

$\phi_{1i}, \lambda_{1i}, R_b, \phi_{2i}, \lambda_{2i}, R_b + H_i$ – spherical coordinates defining spherical prism *i,*

$\psi_i = \arccos\left(\sin\phi_i \sin\phi_P + \cos\phi_i \cos\phi_P \cos\left(\lambda_i - \lambda_P\right)\right)$ – geocentric angle between the attracted point *P* and the volume element $R_i^2 \cos\phi_i d\lambda_i d\phi_i dR_i$,

$\boldsymbol{\rho}^{\mathbf{T}} = [\rho_1, ..., \rho_n]$ is the vector of constant densities of topographic masses,

$\mathbf{t}^{\mathbf{T}} = [t_1, ..., t_n]$ comes from (5) and values t_k (*k=1...n*) are defined as [25]:

$$t_k = G\sum_{i=1}^{m_k}\left(\int_{R_b}^{R_b+H_i} \int_{\phi_{1i}}^{\phi_{2i}} \int_{\lambda_{1i}}^{\lambda_{2i}} \frac{R_i^2 \cos\phi_i}{\sqrt{R_i^2 + R_P^2 - 2R_i R_P \cos\psi_i}} d\lambda_i d\phi_i dR_i\right) \tag{6}$$

The T_κ component may be written by defining the κ region as the one layer of spherical prisms which are limited by spheres with a radius $R_b - T$ - at the bottom and R_b - at the top.

$$T_\kappa(\phi_P, \lambda_P, R_P) = G\sum_{j=1}^{s}\left(\delta_j \int_{R_b-T}^{R_b}\int_{\phi_{1j}}^{\phi_{2j}}\int_{\lambda_{1j}}^{\lambda_{2j}} \frac{R^2\cos\phi_j}{\sqrt{R^2 + R_P^2 - 2R\, R_P \cos\psi_j}} d\lambda_j d\phi_j dR\right) = \mathbf{r}^{\mathrm{T}}\boldsymbol{\delta} \quad (7)$$

where

s – number of spherical prisms of the κ area,

$\phi_{1j}, \lambda_{1j}, R_b - T, \phi_{2j}, \lambda_{2j}, R_b$ – spherical coordinates defining spherical prism *j,*

$\boldsymbol{\delta}^{\mathrm{T}} = [\delta_1, ..., \delta_s]$ is the vector of constant densities of the region κ,

$\mathbf{r}^{\mathrm{T}} = [r_1, ..., r_s]$ comes from (7) and values r_j (*j=1...s*) are defined as [25]:

$$r_j = G\int_{R_b-T}^{R_b}\int_{\phi_{1j}}^{\phi_{2j}}\int_{\lambda_{1j}}^{\lambda_{2j}} \frac{R^2\cos\phi_j}{\sqrt{R^2 + R_P^2 - 2R\, R_P \cos\psi_j}} d\lambda_j d\phi_j dR \quad (8)$$

Considering equations (4), (5) and (7), potential (3) can be now written as follows:

$$T_P = \mathbf{w}^{\mathrm{T}}\mathbf{a} + \mathbf{t}^{\mathrm{T}}\boldsymbol{\rho} + \mathbf{r}^{\mathrm{T}}\boldsymbol{\delta} \quad (9)$$

Evaluation of the disturbing potential and its vertical derivative, according to equation (9) requires calculation of the integrals (6) and (8) and its vertical derivatives. Because the non-closed form of these integrals has not been found yet, a numerical integration is needed. To improve the effectiveness of calculations, not using the numerical methods of integration, Cartesian coordinate system can be used where the solutions of integrals are known. The advantage of implementing such coordinate system is the fact that the model is designed for local use, hence some approximations are acceptable.

Let's define the rectangular Cartesian coordinate system. Its *Z*-axis is directed towards the Zenith and the *X, Y-* axes lay on the horizontal plane and are directed to the North and East. The origin of the coordinate system can be set in the middle of the area. In this case Ω and κ regions are defined as a rectangular grid of rectangular prisms (Fig.2).

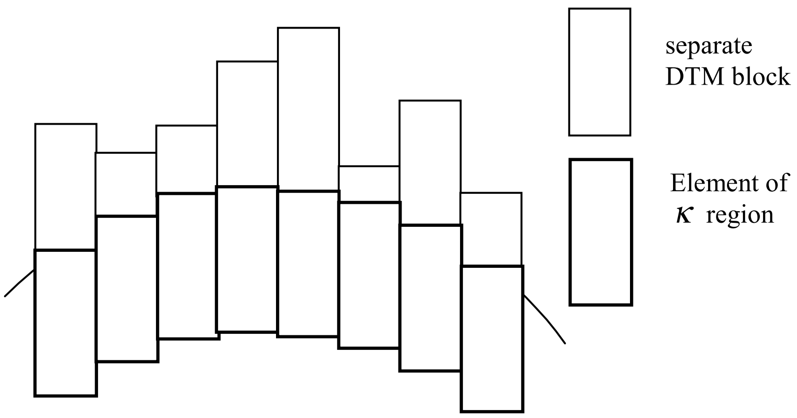

Fig. 2. Ω and κ regions in a Cartesian rectangular coordinate system

With Ω and κ regions defined in this way, the disturbing potential is still given by the equation (9) with some quantities changed. Harmonic spherical polynomials can now be written in Cartesian coordinates as:

$$W(X_P, Y_P, Z_P) = a_0 + a_1 X_P + a_2 Y_P + a_3 X_P Y_P + a_4 Z_P \quad (10)$$

Coefficients t_k and r_j in equations (5) and (7) are now defined by integrals:

$$t_k = G\sum_{i=1}^{m_k}\left(\int_{z_{1i}}^{z_{2i}}\int_{y_{1i}}^{y_{2i}}\int_{x_{1i}}^{x_{2i}}\frac{1}{\sqrt{(x_i - X_P)^2 + (y_i - Y_P)^2 + (z_i - Z_P)^2}}dx_i dy_i dz_i\right) \tag{11}$$

$$r_j = G\int_{z_{1j}}^{z_{2j}}\int_{y_{1j}}^{y_{2j}}\int_{x_{1j}}^{x_{2j}}\frac{1}{\sqrt{(x_j - X_P)^2 + (y_j - Y_P)^2 + (z_j - Z_P)^2}}dx_j dy_j dz_j \tag{12}$$

where

X_P, Y_P, Z_P coordinates of point *P*,

$x_{i1}, x_{i2}, y_{i1}, y_{i2}, z_{i1}, z_{i2}$ coordinates defining rectangular prism *i* of DTM,

$x_{j1}, x_{j2}, y_{j1}, y_{j2}, z_{j1}, z_{j2}$ coordinates defining rectangular prism *j* of κ area.

Solutions of the integrals in equations (11) and (12) and their vertical (*z*) derivatives can be found in many publications [7,16,25].

The disturbing potential model in the form (9), aimed at solving gravity inversion, can be easily used by applying the least-square method. As it was mentioned in the introduction, unknown parameters can be calculated by using different geodetic data, which stand functions of disturbing potential. For the purpose of its importance and availability, the bases of calculations are height anomalies extracted from GPS/levelling measurements and a gravity data. For this kind of data the observation equations will be formulated.

Height anomaly

Following the Bruns formula, a height anomaly can be expressed as a disturbing potential value [29]. Therefore, the observation equation of height anomaly can be written as the observation equation of a disturbing potential.

Hence, we can write:

$$T_P + v_{TP} = \mathbf{f}^{\mathrm{T}}\mathbf{x} \tag{13}$$

where $\mathbf{x}^{\mathrm{T}} = [\mathbf{a}^{\mathrm{T}}, \boldsymbol{\rho}^{\mathrm{T}}, \boldsymbol{\delta}^{\mathrm{T}}] = [a_1,..., a_l, \rho_1,..., \rho_n, \delta_1,..., \delta_s]$ is the unknown vector

$\mathbf{f}^{\mathrm{T}} = [\mathbf{w}^{\mathrm{T}}, \mathbf{t}^{\mathrm{T}}, \mathbf{r}^{\mathrm{T}}] = [w_1,..., w_l, t_1,..., t_n, r_1,..., r_s]$ is the known vector

v_{TP} is an adjustment error.

Gravity data

Gravity anomaly Δg_P is connected with disturbing potential by fundamental equation of physical geodesy [29]:

$$g_P - \gamma_Q = \Delta g_P = \left(-\frac{\partial T}{\partial z}\right)_P + \frac{U_{zz}}{\gamma_Q}T_P \tag{14}$$

where γ_Q is a normal gravity acceleration on telluroid and U_{zz} is its vertical gradient.

Based on this equation, considering disturbing potential model (9), we can write observation equation for the gravity anomaly:

$$\Delta g_P + v_{\Delta gP} = \left(-\mathbf{f}_{\mathbf{z}}^{\mathrm{T}} + \frac{U_{zz}}{\gamma_Q}\mathbf{f}^{\mathrm{T}}\right)_P \mathbf{x} \tag{15}$$

where $\mathbf{f}_{\mathbf{z}}$ is the *Z* derivative of the vector $\mathbf{f}$.

To formulate the equation (15) two vectors should be calculated: $\mathbf{f}_\mathbf{z}$ and $\mathbf{f}$ for each point with measured gravity. To improve calculation speed, quantity $\frac{U_{zz}}{\gamma_Q} T_P$ in the equation (14) for each point can be approximately calculated from existing, less precise quasi-geoid models. Hence, instead of the gravity anomaly in the calculation process a gravity disturbance can be taken. Observation equation for such gravity data will then have the form:

$$\delta g_P + v_{\delta g P} = -\mathbf{f}_\mathbf{z}^\mathrm{T}\mathbf{x} \tag{16}$$

At the origin of local Cartesian coordinate system the equation $\delta g = -\frac{\partial T}{\partial z}$ is certainly true. For distant points from the origin of coordinate system, this equality will turn into approximation. To estimate an error of the approximation, we have to assume that vectors $\mathbf{g}$ and $\boldsymbol{\gamma}$ are directed to the centre of the sphere with radius R=6371 *km*. For the point situated in the distance of 100 *km* from the origin of the coordinate system and with the gravity disturbance of 50 *mGal*, the length of projection of the disturbance on the *Z*-axis will amount 49.994 *mGal*. So, the approximation error is lower than the precision of the gravity measurement and, for a limited area, can be neglected.
Inversion of the gravity data is usually accomplished by adopting a certain reference density model, which we describe as $\boldsymbol{\tau}_0^T = \lfloor \boldsymbol{\rho}_0^T, \boldsymbol{\delta}_0^T \rfloor = \lfloor \rho_1^0, ..., \rho_n^0, \delta_1^0, ..., \delta_s^0 \rfloor$. The searched values are not densities themselves but differences between real, natural densities and the taken reference densities. Additionally, indicating the density model as $\boldsymbol{\tau}^T = \lfloor \boldsymbol{\rho}^T, \boldsymbol{\delta}^T \rfloor = \lfloor \rho_1, ..., \rho_n, \delta_1, ..., \delta_s \rfloor$, the searched differences can be written as $\mathbf{d}\boldsymbol{\tau}^T = \boldsymbol{\tau} - \boldsymbol{\tau}_0$, and the vector of the unknown values as $\mathbf{dx}^T = \lfloor \mathbf{a}^T, \mathbf{d}\boldsymbol{\tau}^T \rfloor$. The equations (13), (15) and (16) will be then written as:

$$\begin{gathered} T_P + v_{TP} = \mathbf{f}^\mathrm{T}\mathbf{dx} + T_P^0 \\ \Delta g_P + v_{\Delta g P} = \left(-\mathbf{f}_\mathbf{z}^\mathrm{T} + \frac{U_{zz}}{\gamma_Q}\mathbf{f}^\mathrm{T} \right)_P \mathbf{dx} + \Delta g_P^0 \\ \delta g_P + v_{\delta g P} = -\mathbf{f}_\mathbf{z}^\mathrm{T}\mathbf{dx} + \delta g_P^0 \end{gathered} \tag{17}$$

where $T_P^0 = \mathbf{f}^\mathrm{T}\mathbf{x}_0$, $\Delta g_P^0 = \left(-\mathbf{f}_\mathbf{z}^\mathrm{T} + \frac{U_{zz}}{\gamma_Q}\mathbf{f}^\mathrm{T} \right)_P \mathbf{x}_0$, $\delta g_P^0 = -\mathbf{f}_\mathbf{z}^\mathrm{T}\mathbf{x}_0$ are the approximate observation quantities determined on the basis of the vector $\mathbf{x}_0^T = \lfloor \mathbf{a}_0^T, \boldsymbol{\tau}_0^T \rfloor$, where the vector $\mathbf{a}_0$ is *l*-dimension zero vector .

The formulated equations (17), for the observations series may be written in a more convenient way as:

$$\mathbf{v} = \mathbf{Adx} - \mathbf{L} \tag{18}$$

where $\mathbf{v}^T = \lfloor v_{TP}, ..., v_{\Delta g P}, ..., v_{\delta g P}, ... \rfloor$ is the adjustment errors vector,
$\mathbf{L}^T = \lfloor T_P - T_P^0, ..., \Delta g_P - \Delta g_P^0, ..., \delta g_P - \delta g_P^0, ... \rfloor$ is a known observation vector and $\mathbf{A}$ is design matrix of known coefficients.

When the given weight matrix **P**, which was defined by the reciprocal of the observational errors squares, the system of equations (18) can be solved by general condition of the least squares in the form:

$$\mathbf{v}^T\mathbf{P}\mathbf{v} = \min \tag{19}$$

We have to realize the estimated densities of topographic masses will not be correct. It is caused by the fact that the base of modelling is the surface gravimetric data which does not inherit density depth resolution. In other words, the disturbing masses may be situated on various depths and give the same outcome which are gravimetric anomalies on the surface. To overcome this difficulty, various techniques are used. Li and Oldenburg [15] suggested the approach that will be used in the presented solution. It requires a supplement condition to be put on the determined densities $\mathbf{d\tau}$:

$$\phi_m(\tau) = \mathbf{d\tau}^T \mathbf{W_\tau} \mathbf{d\tau} = \min \tag{20}$$

Where $\mathbf{W_\tau}$ is the model weighting matrix, the purpose of which is to strengthen or to weaken the influence of the designated values in various regions of the model domain on the data values. Introducing the condition (20) gives certain control over the inversion process. The authors suggest establishing the weight values by using the function $\phi_m(\tau)$ in the form [15]:

$$\begin{aligned}\phi_m(\tau) &= \alpha_S \int_V w_S \{w(z)[\tau - \tau_0]\}^2 dv \\ &+ \alpha_x \int_V w_x \left\{\frac{\partial w(z)[\tau - \tau_0]}{\partial x}\right\}^2 dv \\ &+ \alpha_y \int_V w_y \left\{\frac{\partial w(z)[\tau - \tau_0]}{\partial y}\right\}^2 dv \\ &+ \alpha_z \int_V w_z \left\{\frac{\partial w(z)[\tau - \tau_0]}{\partial z}\right\}^2 dv\end{aligned} \tag{21}$$

where functions w_S, w_x, w_y, w_z are spatially dependent weighting functions, $\alpha_S, \alpha_x, \alpha_y, \alpha_z$ are coefficients that determine the relative importance of different components in the function $\phi_m(\tau)$ and $w(z)$ is a depth weighting function.

The most important is a depth weighting function $w(z)$, which, according to the authors, should have the following form for gravimetric data :

$$w(z) = \frac{1}{(z - z_0)^{\beta/2}} \tag{22}$$

where β should be in the range of $1.5 < \beta \leq 2.0$ and z_0 depends on cell size of the model discretization and the data height.

Recording the condition (20) for the whole vector of the unknown, the unknown polynomial coefficients (10) have to be included in the vector. The $\mathbf{W_a}$ model weighting matrix will be assigned to these coefficients and the condition (20) will be now written as:

$$\mathbf{dx}^T \mathbf{W_x} \mathbf{dx} = \min \tag{23}$$

where $\mathbf{W_x} = \begin{bmatrix} \mathbf{W_a} & \mathbf{0} \\ \mathbf{0} & \mathbf{W_\tau} \end{bmatrix}$, and $\mathbf{W_a}$ is the zero matrix.

Least square objective function can now be written as:

$$\mathbf{v}^T \mathbf{P} \mathbf{v} + \mathbf{dx}^T \mathbf{W_x} \mathbf{dx} = \min \tag{24}$$

The equation set (18), including the condition (24) is solved in the following way:

$$\mathbf{x} = \left(\mathbf{A}^T \mathbf{P} \mathbf{A} + \mathbf{W_x}\right)^{-1} \mathbf{A}^T \mathbf{P} \mathbf{L} \tag{25}$$

It has to be mentioned that this solution may be found in the iteration process.

TEST CALCULATIONS

The object and test data

The test calculations were performed in the part of Lower Silesia region. The area of elaboration spreads from the southern borderline of Poland to the parallel of the latitude $51^o\,30'$ (about 155 *km*) and from the meridian 16^o to the meridian 18^o (about 142 *km*). Mostly, this is a low-lying area. The southern part of the area contains partially the Sudetes Foreland and the Sudetes Mountains. To perform the calculations, a right-rectangular coordinate system was introduced. The origin of the reference is handled at the point $B = 50.8^o$, $L = 17^o$ (approximately in the centre of the elaborated area). The *XY* plane is tangent to the geoid and the *Z*-axis is directed to the Zenith.

For the purpose of calculations 7964 points were used with previously measured gravity that referred to the International Gravity Standardization Network 1971 (IGSN71), available from the Polish Geological Institute as well as 26 points of the POLREF network, with known both ellipsoidal and normal heights. Figure 3 shows locations of the POLREF network points in the terrain. Inside the area marked with the dashed line, gravimetric data applied in the calculations were situated.

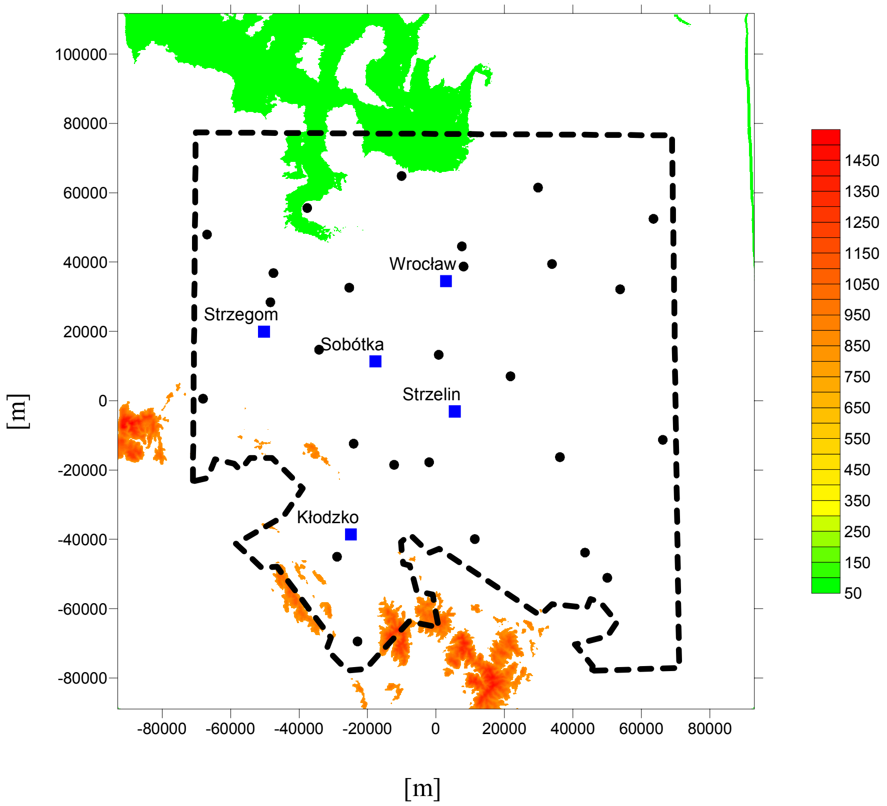

points of POLREF network

the border of the area from which the gravimetric data have been used

Fig. 3. Location of gravity points and the POLREF network points

The Ω region for all test calculations went about 20 km behind the area where the results of gravity measurements had been given. This area is shown on the Fig. 3. The region was divided into 1600 zones of constant density of topographic masses. A particular zone was the rectangle at the size of ca. 5×4.3 km. The κ region was defined as the set of rectangular prisms that constitute the layer that has the constant depth of 32 km (the average depth of the compensation surface in the Lower Silesia region [6]). Single cell of the κ region corresponded to the appropriate zone of the Ω region by its horizontal size and position. For each gravity point, gravity disturbance was calculated with the use of approximated quasi-geoid model, built on the base of the POLREF network points. Therefore observation equations for gravity data were built according to the equation (16).

The accuracy of height anomalies determination and the assessment of minimal density of points with the designated GPS/levelling heights

First, the series of 26 calculations was taken. In each calculation set, one of the POLREF points was taken as the unknown and the other 25 points were treated as data points. Such approach was implemented to assure a minimal distance between unknown and known points. In calculation the DTM at density of 500 m was used.

Figure 4 presents d_ζ differences in centimetres, between quasi-geoid heights calculated from the model and its "theoretical" heights, for each of 26 points. The largest differences appear at points situated close to the border of the elaboration area. Reducing the accuracy of height anomalies determination near the border of the area from which the data was extracted is the expected phenomena and is called the edge effect. The size of the edge effect confirms the usefulness of the suggested area. In the Figure 4, the area where the edge effect is significant was separated by a green dashed line and constitutes the external part of the whole area. The internal part defines a certain sub-area, in which the calculated height anomalies are very close to their "theoretical" values. The sub-area will be called the area of the suggested method efficiency. Points situated inside the efficiency area may be used for estimating the precision of the method.

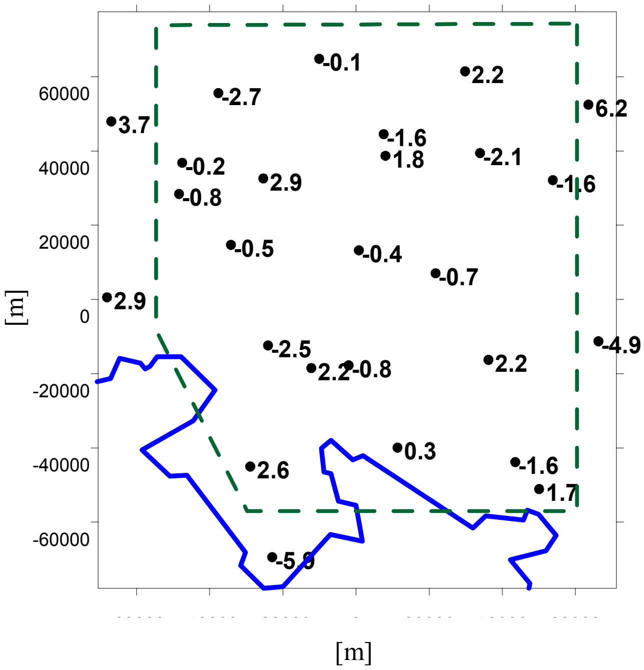

Fig. 4. d_ζ **differences between quasi-geoid heights calculated from the model and its "theoretical" values, in centimetres**

Accuracy parameters determined on the strength of d_ζ differences for these points are presented in the Table 1 and indicated as the variant V1.

Table 1. Accuracy parameters in centimetres for the variant V1

	V1 $[cm]$
DTM resolution $[m]$	500
maximal error value $\max\lvert d_\zeta \rvert$	2.9
mean square error $m_\zeta = \sqrt{\frac{\sum d_\zeta^2}{n}}$	1.7
mean error $m_{\lvert\zeta\rvert} = \frac{\sum \lvert d_\zeta \rvert}{n}$	1.5

To sum up the presented results briefly, we have to emphasis the high accuracy of the determined height anomalies. We must notice that the test calculations refer to the POLREF network points. The accuracy of height anomalies of that points is estimated at the level of $m_{\zeta}^{H} \cong \pm 2\,cm$ [13]. As far as the mean square error is concerned, the gained outcomes are on the accuracy level of GPS/levelling height anomalies of the POLREF network points. Such results were obtained using gravimetric data from the region that goes only 15 *km* behind the efficiency area. It shows there is only slight edge effect of the presented approach.
In the framework of the second calculation test, the case where the distance between known points is larger can be analysed. From several series of calculations such a variant was chosen where the number of known GPS/levelling points is minimal and the results are as good as in the previous test. Increasing the number of the known points does not influence the results greatly but reducing the number of these points decreases the model accuracy. Finally, eight points of the POLREF network were taken as the data points and the other points were treated as test points. The Figure 5 presents a location of the data and test points and the results of test calculations described as d_{ζ} difference.

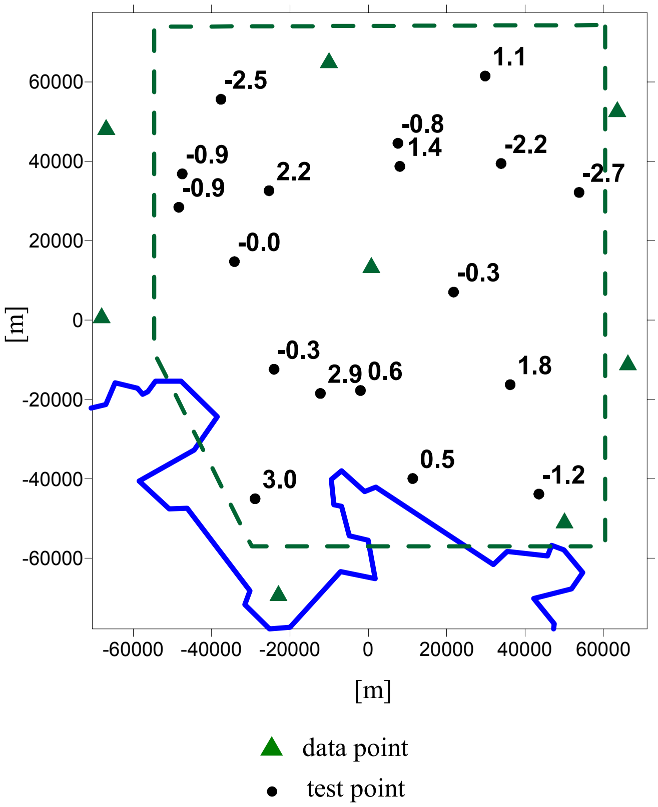

Fig. 5. The location of the data and test points as well as the differences d_{ζ} between quasi-geoid heights calculated from the model and its "theoretical" values, in centimetres (variant V2)

As it may be noticed in the Fig. 5 the majority of data points is situated outside the efficiency area. This area has not been changed. As in the previous case, for the purpose of calculations DTM with density of 500 *m* was used. The parameters of the accuracy for this variant which were determined on the basis of differences d_{ζ} are presented in the Table 2 and indicated as V2.

Table 2. Accuracy parameters in centimetres determined for the variant V2

	V2 $[cm]$
DTM resolution $[m]$	500
maximal error value $\max\lvert d_\zeta \rvert$	3.0
mean square error $m_\zeta = \sqrt{\frac{\sum d_\zeta^2}{n}}$	1.7
mean error $m_{\lvert\zeta\rvert} = \frac{\sum \lvert d_\zeta \rvert}{n}$	1.4

On the basis of Fig. 5 the maximum distance between data points may be evaluated as 50-60 *km*. However, there are particular requirements for the localization of these points: points which have their anomalies determined have to be situated among data points. It will be also reflected in the results of test calculations presented in the further part of this paper.

The evaluation of DTM resolution influence on the accuracy of height anomalies determination

To evaluate DTM resolution influence on the interpolation results the additional calculations were made for data and test points situated as it is shown in the Fig. 5 (variant V2). For the purpose of calculations, DTM with density of 150, 250, 500, 750 and 1000 *m* was used. Accuracy parameters determined for specific resolutions are presented in the Table 3.

Table 3. Accuracy parameters in centimetres determined for various DTM resolutions

	V3 $[cm]$				
DTM resolution $[m]$	150	250	500	750	1000
maximal error value $\max\lvert d_\zeta \rvert$	3.1	3.4	3.0	2.8	2.6
mean square error $m_\zeta = \sqrt{\frac{\sum d_\zeta^2}{n}}$	1.7	1.8	1.7	1.7	1.7
mean error $m_{\lvert\zeta\rvert} = \frac{\sum \lvert d_\zeta \rvert}{n}$	1.4	1.4	1.4	1.4	1.4

We have to mention that the original DTM was the model with resolution of 150 *m*. On the strength of this model, DTM nets with other resolutions were generated.
The results got for the analyzed area presented in the Table 3 show that the DTM resolution in the range of 150*m* to 1000*m* does not influence the determined height anomalies. However, we have to notice that this area is mainly low lying and only its small part may be considered as a piedmont or mountainous region, where the significant influences can be expected.

The assessment of the accuracy of height anomalies determination for points situated near the border of the elaboration area (edge effect)

In the computation of variants V2 and V3 data points are situated near the elaboration area border. Therefore, the edge effect can not be assessed when the minimal number of data points is used. For the proper evaluation, data points were moved close to the centre of elaboration area so that the test points were situated outside the efficiency area. Figure 6 presents the location of data and test points as well as the results of calculations for DTM with the resolution of 500 *m*.
Shifting data points in this case caused the change of the efficiency area border. It is presented explicitly that the points on which height anomalies are determined should be situated among data points. On the basis of these computations we may assess not only accuracy parameters for points situated inside the efficiency area, but also such parameters for points lying outside the efficiency area.

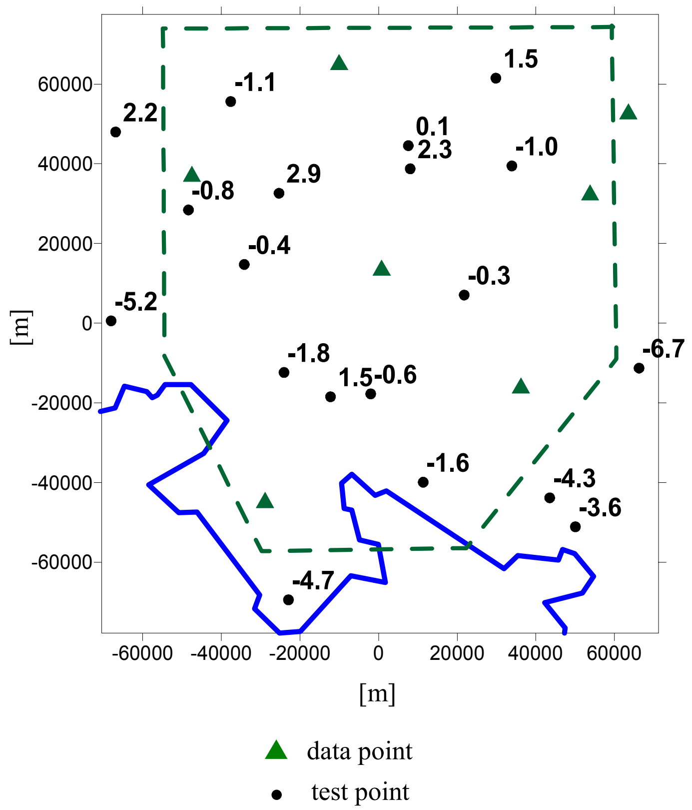

Fig. 6. The location of data and test points and d_ζ differences between quasi-geoid heights calculated from the model and its "theoretical" values, in centimetres (variant V4)

Accuracy parameters for the both groups of points are shown in the Table 4. These values were determined for variant V1 and for the setting of data and test points as shown in the Fig. 6. The outcomes of these computations are given in the Table for and marked as the variant V4.

Table 4. Accuracy parameters in centimetres determined for points situated outside and inside the efficiency area

	V1 $[cm]$		V4 $[cm]$									
DTM resolution $[m]$	500		150		250		500		750		1000	
	in	out	in	out	in	out	in	out	in	out	in	out
maximal error value $\max\|d_\zeta\|$	2.9	6.2	2.9	6.7	2.9	6.7	2.9	6.7	2.9	6.7	2.9	6.7
mean square error $m_\zeta = \sqrt{\frac{\sum d_\zeta^2}{n}}$	1.7	4.9	1.4	4.5	1.5	4.7	1.5	4.7	1.5	4.6	1.5	4.5
mean error $m_{\|\zeta\|} = \frac{\sum \|d_\zeta\|}{n}$	1.5	4.7	1.2	4.2	1.2	4.5	1.2	4.5	1.2	4.4	1.2	4.3

Results in the Table 4 indicate that errors of height anomalies determination for points placed outside the efficiency area are several times bigger than the errors of height anomalies determination for points lying inside this area. To reduce this error, global geopotential model EGM96 was implemented to calculations by remove-restore method. The outcomes of these computations for the DTM with density of 500 *m* are presented in the Figure 7.

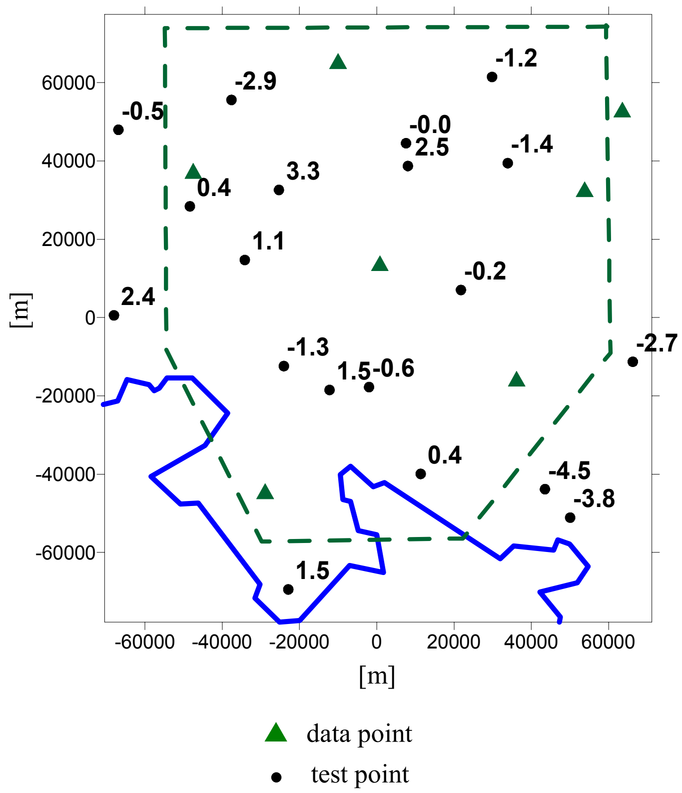

Fig. 7. The location of the data and test points and differences d_ζ between quasi-geoid heights calculated from the model and its "theoretical" values with the use of EGM96 model, in centimetres (variant V4)

Table 5 shows accuracy characteristics of this variant of test calculations performed for various DTM densities. This variant is called V5.

Table 5. Accuracy parameters in centimetres determined for points situated outside and inside the efficiency area using EGM96 model

	V5 $[cm]$									
DTM resolution $[m]$	150		250		500		750		1000	
	in	out	in	out	in	out	in	out	in	out
maximal error $\max\lvert d_\zeta \rvert$	3.1	4.1	3.2	4.1	3.3	4.5	3.1	4.3	3.1	4.1
mean square error $m_\zeta = \sqrt{\frac{\sum d_\zeta^2}{n}}$	1.6	2.8	1.6	2.7	1.6	2.9	1.6	3.0	1.6	2.8
mean error $m_{\lvert\zeta\rvert} = \frac{\sum \lvert d_\zeta \rvert}{n}$	1.3	2.5	1.3	2.4	1.3	2.5	1.3	2.6	1.3	2.5

The presented outcomes for the variants V4 and V5 first of all confirm the lack of significant influence of DTM in the range of 150-1000m on the results obtained for the investigated area. Furthermore, applying global geopotential model practically does not influence the determined quasi-geoid heights inside the efficiency area in a considerable way. On the other hand, it is crucial to reduce the edge effect. In the rendered example all errors have been reduced approx. by 40%. It supports using global geopotential models in the suggested method.

Determination of topographic masses density

The determined models of topographic masses density distribution were evaluated by comparing the results of test calculations with the fragment of the map of rock slab density above the sea level, which was made in the scale 1:1000000 [12]. According to authors, this map uses densities of topographic masses evaluated with the mean standard deviation of ± 0.11 $g \cdot cm^3$. This map allowed to prepare the draft of topographic masses presented in the Figure 8.

Figure 8 shows that the elaboration area with regard to topographic masses density may be divided into two parts, i.e. mountainous part which has higher density and low lying part with lower density. Parts are separated by the line of the Sudetes border fault line. On the north-east, low side of the fault the regions with high density prevail and they encompass Ślęża Massif, western part of Niemcza-Strzelin Hills (south-east of Strzelin) and Strzegom precincts.

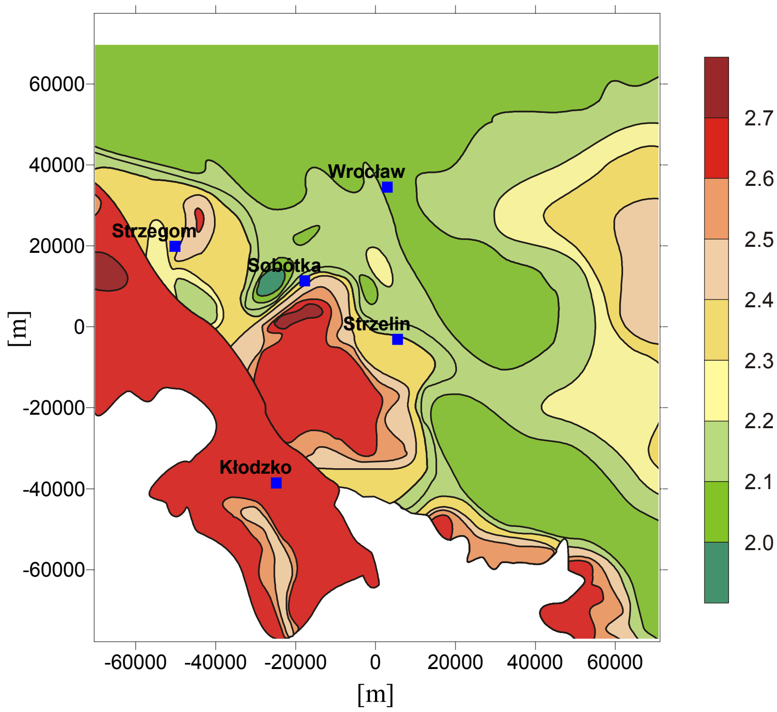

Fig. 8. The draft of the topographic masses density made on the basis of the map of density of rock slab above sea level [12]

Test computations were made for two variants. For both variants the reference density model for the κ area amounted $\boldsymbol{\tau}_0^{\kappa} = 0\,\mathrm{g \cdot cm}^3$ and for Ω area it was $\boldsymbol{\tau}_0^{\Omega} = 2.20\,\mathrm{g \cdot cm}^3$. This value is close to the average density of topographic masses for Poland which is estimated as $2.17\,\mathrm{g \cdot cm}^3$ [12]. These two variants differ in some parameters that define weight matrix $\mathbf{W}_{\boldsymbol{\tau}}$. DM1 variant assumes that weights for Ω area are the same for each zone. Due to the fact that the whole area was divided into 1600 zones that differ only in the terrain altitude, in order to determine weights for this variant the equal height of all zones was adopted and it was evaluated as the average height of the terrain on the tested area. DM2 variant on the contrary allows for differences in the terrain altitude in the each zone of Ω area. For this reason, weights are different for each zone.
Regarding the same sizes and depth of location of the κ area components, weights for the each component of the area will be the same.
Figure 9 renders a density model determined for DM1 variant. In calculations, the following, remaining values of the function $\phi_m(\tau)$ were used: $w_x = w_y = w_z = 1$ and $w_S = \begin{cases} 0.00001\, for\ \Omega \\ 0.000025\, for\ \kappa \end{cases}$, the coefficients $\alpha_x = \alpha_y = \alpha_z = 0$ and $\alpha_S = 0.00001$, $\beta = 2$, $z_0 = 500\,m$. Such way of weighting and the values of the function component presented above $\phi_m(\tau)$ were used in all calculations whose results are presented above.

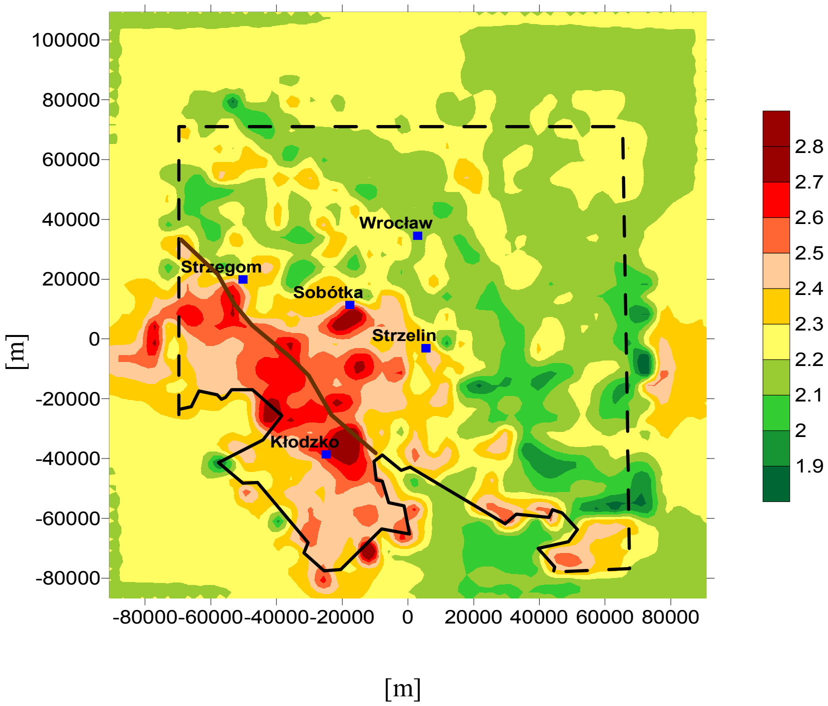

Fig. 9. The determined densities of tropospheric masses after accepting the same heights for all the zones in the Ω area for the weight function (DM1 variant)

Comparing Figures 8 and 9, we may notice that the greatest changes of topographic masses density in the Sudetes region, Ślęża Massif and Niemcza-Srzelin Hills were spotted in the modelling process. However, the determined densities feature much higher density than the theoretical values of density. Locally, they also diverge from them (e.g. in the southern part of Kłodzko Valley). The line of Sudetes border fault that separates flat areas with lower density from mountainous terrains with the much higher density and which is very evident in the Figure 8, is hardy noticeable in the Figure 9. For the low lying areas (Wroclaw precincts), where the density of topographic masses only slightly differs from the adopted reference density model, the determined densities in principle do not reflect the theoretical densities.

In the case of DM2 variant various terrain altitudes of each zone were taken into account . Implementing different heights to weight function calculations also required the modification of other components of the $\phi_m(\tau)$ function. The calculations for DM2 were made taking the following assumptions: the functions $w_x = w_y = w_z = 1$ and

$$w_S = \begin{cases} 0.002 \; for \; \Omega \\ 0.013 \; for \; \kappa \end{cases}$$, the coefficients $\alpha_x = \alpha_y = \alpha_z = 0$ and $\alpha_S = 0.00001$, $\beta = 2$, $z_0 = 5000\,m$.

The density model determined for this variant is presented in the Figure 10.

Comparing Figures 9 and 10 we may claim that including various terrain heights of zones within the Ω area in the weight function, did not considerably influence the results of modelling. Therefore, it is not important for the testing area.

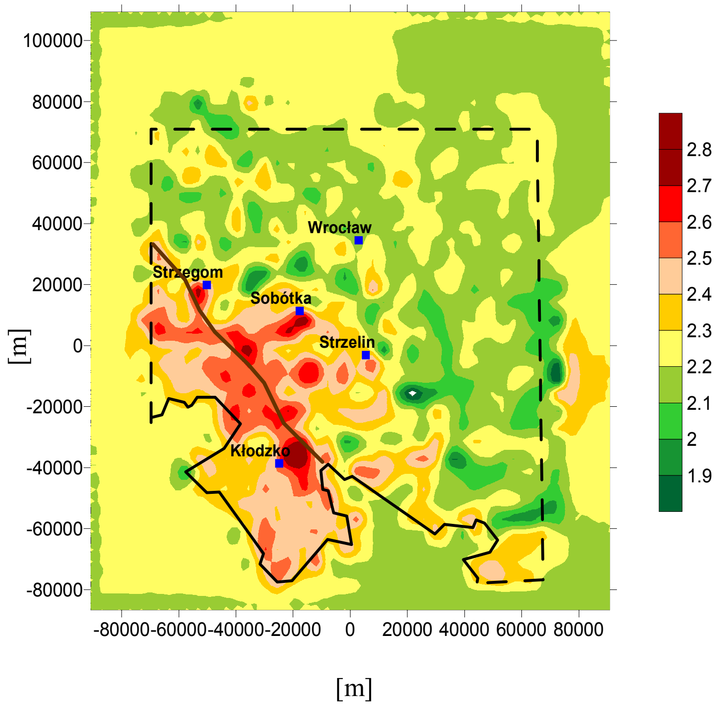

Fig. 10. The determined densities of topographic masses including zone height differences in the Ω region for the weight function (variant DM2)

Moreover, the fragment of the map of density of the rock slab above the sea level presented in the Figure 8 was digitized. Digital data collected in this process allowed to compute mean density errors for each of the variants. These errors were calculated according to the formula $m_{\tau^\Omega} = \sqrt{\frac{\sum(\Delta\tau)^2}{n}}$, where $\Delta\tau$ is the difference of the determined and theoretical density (received from map digitization) for each zone and n is the number of zones. These errors are shown in the Table 6.

Table 6. Errors of determined topographic masses densities in g/cm^3

Variant	DM1	DM2	Constant density (2.20)
$m_{\tau^\Omega} = \sqrt{\frac{\sum\Delta\tau^2}{n}}$	0.145	0.153	0.194

The last column of the Table 6 includes m_{τ^Ω} error for the reference density model $\boldsymbol{\tau}_0^\Omega = 2.20\,\mathrm{g}\cdot\mathrm{cm}^3$.

The accuracy parameters presented in the Table 6 confirm the deficiency of significant discrepancy between DM1 and DM2 variants.

To summarise this part of test calculations briefly, I would like to emphasise that data on topographic masses densities which I applied here come from the map in the scale of 1:1000000. This map was drawn using densities determined with the precision of $\pm 0.11\,\mathrm{g}\cdot\mathrm{cm}^3$. Such data allow to make only general evaluation of the results of densities modelling. This evaluation states clearly that the applied disturbing potential model facilitates interpolation of height anomalies with the simultaneous modelling of topographic masses densities mainly in the mountainous areas. To determine the accuracies of densities determination in an unambiguous way, the further analyses have to be made both on theoretical and real data.

CONCLUSIONS

This work presents the method for local determination of quasi-geoid heights which uses not reduced data. Such approach allows to omit the influence of determined corrections inaccuracies and reductions that are implemented to the input data on the final outcome of calculations. Although it uses DTM data which are the source of topographic correction commonly introduced in the classical methods, in fact the model quality requirements seem to be much lower. The influence of DTM with the resolution of $150 \times 150\, m$ up to $1000 \times 1000\, m$ on the determined height anomalies have not been proven for the tested area. But we still have to take into account that the tested area is mainly low lying and only in parts it covers piedmont and low mountains terrains. Because the greatest influence of DTM accuracy on the calculation results is expected in the mountainous areas, the presented results should be verified in the area that is in total mountainous.

The test calculations showed the high accuracy of height anomalies determined by this method. For the tested area agreement of the modeled quasi-geoid heights with GPS/leveling designations was reached at the level of $\pm 1.7\, cm$ (mean square error). It should be noticed that gravity data used for the calculations covers only a small elaboration area (Figure 3), and good results were obtained just about 15 *km* from its border (small edge effect). It is an interesting property which particularly supports such solution in case of lack of the gravity data in the large regions outside the area of interest, which is needed in Stokes integration method (e.g. for border areas).

The suggested method uses various surveying data. The basis of calculations are still gravimetric data, GPS/levelling height anomalies and digital terrain model. It limits the scope of using this method to the areas for which such data are available. The situation of points with the known GPS/levelling heights is crucial. The highest accuracy of height anomalies determination is reached on the area where the known points are situated. In order to increase the interpolation precision for the points located outside this area, it is effective to use the global geopotential model in the remove-compute-restore technology.

To summarise this part of work which is connected with topographic masses densities modelling, we have to mention that for the purpose of researches the test data were used. They were taken from the map of density of the rock slab above the sea level in the scale of 1:1000000. The test data allow to make only general evaluation of densities modelling results. This evaluation shows that the suggested solution permits height anomalies determination with simultaneous modelling of topographic masses densities. However, unequivocal evaluation of accuracies determined with this method requires further analyses that use more precise test data.

Finally, it is worth mentioning that discretizing density functions ρ and δ and selection of various weight functions $w(z)$, facilitates generation of many variants of disturbing potential model. It indicates the necessity of conducting wider and more precise researches of the rendered solution.

REFERENCES

1. Bajracharya S., Sideris M.G., 2005. Density and gravity interpolation effects on Helmert geoid determination. Geodezja i Kartografia 54 (2), 51-68.
2. Bajracharya S., Sideris M.G., 2005. Terrain-aliasing effects on gravimetric geoid determination. Geodezja i Kartografia 54(1), 3-17.
3. Baran L. W., 1999. Reference Networks. Polish National Report on Geodesy 1995–1999. Polish National Committee for International Union of Geodesy and Geophysics.
4. Blakely R. J., 1995. Potential Theory in Gravity and Magnetic Applications. Cambridge University Press.
5. Brovar W.W., 1983. Gravity field in problems of engineering geodesy. Science, Moscow.
6. Fajklewicz Z., 1972. Zarys geofizyki stosowanej [An Outline of Applied Geophysics]. Wydawnictwo geologiczne, Warszawa – reference book [in Polish].
7. Forsberg R., Tscherning C.C., 1997. Topographic effects in gravity field modelling for BVP. Geodetic Boundary Value Problems in view of the one centimetre geoid. Lecture notes in earth science, Springer-Verlag Berlin Heidelberg.
8. Heiskanen WA., Moritz H., 1967. Physical geodesy. Freeman, San Francisco.
9. Hofmann-Wellenhof B., Moritz H., 2005. Physical geodesy. Springer Wien New York 2005.
10. Huang J., Vaniček P., Pagiatakis D., Brink W., 2001. Effect of topographical density on geoid in the Canadian Rocky Mountains. Journal of Geodesy 74, 805-815, Springer-Verlag.
11. Jekeli C., Serpas J.G., 2003. Review and numerical assessment of the direct reduction in geoid determination. Journal of Geodesy 77, 226-239, Springer-Verlag.
12. Królikowski C., Polechońska O., 2005. Quality of crustal density data in Poland. Workshop II: Summary of the project on a cm geoid in Poland 16-17 November 2005, Warsaw.
13. Kryński J., Osada E., Figurski M., 2005. GPS/levelling data In Poland In view of precise geoid modelling. Workshop II: Summary of the project on a cm geoid in Poland 16-17 November 2005, Warsaw.

14. Kuhn M., 2003. Geoid determination with density hypotheses from isostatic models and geological information. Journal of Geodesy 77, 50-65, Springer-Verlag.
15. Li Y., Oldenburg D. W., 1998. 3-D inversion of gravity data. Geophysics 63(1), 109-119.
16. Nagy D., 1966. The gravitational attraction of right angular prism. Geophysics 31, 362-371.
17. Nahavandchi H., 2000. The direct topographical correction in gravimetric geoid determination by the Stokes-Helmert method. Journal of Geodesy 74, 488-496, Springer-Verlag.
18. Omang O. C.D., Forsberg R., 2000. How to handle topography in practical geoid determination: three examples. Journal of Geodesy 74, 458-466, Springer-Verlag.
19. Sansò F. Rummel (Eds.), 1997. Lecture Notes in Earth Sciences. Geodetic Boundary Value Problems in View of the One Centimeter Geoid. Springer-Verlag Berlin Heidelberg.
20. Sjöberg L.E., 2000. Topographic effects by the Stokes-Helmert method of geoid and quasi-geoid determination. Journal of Geodesy 74, 255-268, Springer-Verlag.
21. Sjöberg L.E., 2003. A computational scheme to model the geoid by the modified Stokes formula without gravity reductions. Journal of Geodesy 77, 423-432, Springer-Verlag.
22. Sjöberg L.E., 2004. The effect on the geoid of lateral topographic density variations. Journal of Geodesy 78, 34-39, Springer-Verlag.
23. Sjöberg L.E., 2005. A discussion on the approximations made in the practical implementation of the remove–compute–restore technique in regional geoid modelling. Journal of Geodesy 78, 645-653, Springer-Verlag.
24. Sjöberg L.E., Nahavandchi H., 1999. On the indirect effect in Stokes-Helmert method in geoid determination. Journal of Geodesy 73, 87-93, Springer-Verlag.
25. Smith D.A., Robertson D.S., Milbert D.G., 2001. Gravitational attraction of crustal masses in spherical coordinates. Journal of Geodesy 74, 783-795, Springer-Verlag.
26. Tarantola A., 2005. Inverse Problem Theory and Methods for Model Parameter Estimation. Society for Industrial and Applied Mathematics, Philadelphia.
27. Teleford W.M., Geldart L.P., Sheriff R. E., 1990. Applied Geophysics Second Edition. Cambridge University Press – reference book.
28. Torge W., 1989. Gravimetry. Walter de Gruyter, Berlin, New York.
29. Torge W., 2001. Geodesy. Walter de Gruyter, Berlin, New York.
30. Trojanowicz M., 2002. Local modelling of the disturbing potential with the use of quasigeoid heights, gravimetric data and digital terrain model. Geodezja i Kartografia t. LI, z.1-2, 35-43.
31. Tscherning C.C., 2001. Geoid determination after first satellite gravity missions. Paper prepared at the occasion of the 70 birthday of Wolfgang Torge.
32. Tsoulis D., 2001. Terrain correction computations for a densely sampled DTM in Bavarian Alps. Journal of Geodesy 75, 291-307, Springer-Verlag.
33. Vaniček P., Christou N.T., 1994. Geoid and its geophysical interpretations. CRC Press, Inc.

Accepted for print: 5.11.2007

Marek Trojanowicz
Institute of Geodesy and Geoinformatics
Wrocław University of Environmental and Life Sciences
Grunwaldzka 53, 50-357 Wrocław, Poland
trojanowicz@kgf.ar.wroc.pl